JOURNAL OF MATERIALS SCIENCE 28 (1993) 121–128

# Tyranno (Si–Ti–C–O) fibres

## Part I *Surface structure studied by scanning tunnelling microscopy*

N. M. D. BROWN, H. X. YOU
*Surface Science Laboratory, Department of Applied Physical Sciences, University of Ulster, Coleraine, County Londonderry BT52 1SA, UK*

The surface structure of the Tyranno (Si–Ti–C–O) fibres in the as-received condition and after thermal desizing treatment has been characterized by scanning tunnelling microscopy (STM) and scanning electron microscopy (SEM). The combination of ultra-high-resolution STM and conventional SEM allows a comprehensive study of the surface structural details of Tyranno fibres from the submicrometre down to nanometre scales or better. The micro-filamentary structure which appears in the scanning electron micrographs was also observed by STM, at much higher magnifications, i.e. on or below the nanometre scale, from the sample surfaces before and following the desizing treatment used. After the removal of the surface size coating from the as-received Tyranno fibre, significant structural changes were observed by STM in the detailed surface topography. These changes were most obvious in the micro-filamentary and granular structure seen. The surface of the size-free Tyranno fibre is predominately non-crystalline and amorphous in structure at scales at or below a nanometre. One of the frequent micro-filamentary, or fibrillar, structures observed by STM on the thermally desized Tyranno fibre surfaces, i.e. those structural features narrow in width and curved in form, are believed to be derived from the initial structure of the polymeric chains present in the fibre at the onset of the processing of the precursor material.

## 1. Introduction

Tyranno fibre (Ube Industries Ltd) is a new type of silicon carbide (SiC) fibre containing titanium as well as oxygen, made by pyrolysis of the organometallic polymer precursor, polytitanocarbosilane (PTC), synthesized from polycarbosilane (PC) and titanium tetrabutoxide [1, 2]. The melt-spun PTC fibre is cured in air below 200 °C and then heat treated continuously at a temperature ranging from 800–1500 °C in a nitrogen atmosphere to obtain continuous Si–Ti–C–O fibres with typical atomic ratios of Si:C:O:Ti = 1:1.32:0.96:0.04 [2, 3]. These fibres are found to be significantly improved in mechanical properties over other polymer-based pyrolytically formed SiC fibres, i.e. of higher tensile strength, higher tensile modulus, with excellent compatibility for use in composites, and more importantly, higher thermal stability [2–6]. Such strength-improved properties make Tyranno fibres very useful as reinforcement for composites, particularly for elevated temperature applications. Clearly, these properties meet the demand for the development and further use of advanced matrix composites of diverse industrial utility.

It is well established that these various advantageous properties of Tyranno fibre are attributable to the retention of an amorphous structure in the fibre even at temperatures up to 1500 °C [2, 5]. Hence, it appears that the mechanical properties of Tyranno fibre are strongly associated with the actual fibre composition and the processing-dependent fibre microstructure. On the other hand, the surface composition and topography of the fibre plays an important role in the adhesion between the fibre and the surrounding matrix in a Tyranno-based composite material. Better understanding of fibre microstructure is therefore essential so as to improve the overall performance of the fibres themselves and the associated composites.

Recently, the structure and properties of Tyranno-type Si–Ti–C–O fibres, their composites and polytitanocarbosilane precursors have been the subjects of a number of studies by means of X-ray diffraction [3–7], electron microscopy (SEM and TEM) [4, 5], magic-angle spinning nuclear magnetic resonance (MAS–NMR) [3, 6] and infrared spectroscopy [6–8]. The SEM study of the Tyranno fibres in the as-received condition and after heat treatment at 1300 °C has shown that their external surfaces appear smooth and featureless at the magnifications used [4]. On the other hand, high-resolution transmission electron micrographs of heat-treated Si–Ti–C–O fibres have shown the existence of β-SiC microcrystallites in some fibre regions [5]. X-ray diffraction has shown the formation of crystalline β-SiC and/or TiC regions in the fibres [5, 7], with the corresponding crystallite size

0022–2461  

~ 1.0 nm [7]. This latter parameter has been found to at least double after the commonly used high-temperature heat treatment (up to 1300 °C) in an inert atmosphere [4, 5].

As far as the crystallite size in the Tyranno fibre is concerned, the observation by electron microscopy (SEM or TEM) of the ultra-microcrystalline structures less than several nanometres in size may be beyond the limitations imposed by their typical imaging resolution capabilities. For instance, SEM resolves relatively large topographical structures with a typical resolution of > 10 nm; TEM studies of thin films (~ 10 nm thick) give a lateral resolution of > 0.2 nm [9]. However, TEM is not a surface topographical probe. In this regard, verification of an amorphous state for the structure of the Tyranno fibre at scales less than a few nanometres by electron microscopy is obviously difficult, particularly when structural details are required. On the other hand, neither X-ray diffraction nor nuclear magnetic resonance, etc., as bulk average structural methods, are direct surface imaging techniques. Therefore, to elucidate the surface details of typical Tyranno fibres, at near nanometre scales or less, a direct surface imaging technique with the required ultra-high resolution is needed. Scanning tunnelling microscopy (STM) is just such a method.

Scanning tunnelling microscopy, since its first appearance in 1982 [10], has proved to be a powerful tool, especially in the determination of either ordered or disordered surface structure at ultra-high resolution, i.e. in scales from nanometres down to a tenths of a nanometre, whether in vacuum, air or liquid environments. Initially, STM techniques were applied mainly to metal and semiconductor surfaces. More recently, this method has been turned directly to studies of other materials of industrial interest. For example, scanning tunnelling microscopy has been used successfully to reveal local atomic structures with graphitic symmetry on the surfaces of PAN-based carbon fibres in air [11] and to monitor the ultimate surface quality of tungsten carbide (WC–Co) ball bearings [12]. Importantly, STM imaging is a direct surface probe, without the need for surface decoration, staining or the replication techniques sometimes required in electron microscopy, and is applicable to any materials of reasonable electrical conductivity. Tyranno fibre is just such a material. Moreover, given its intrinsic operational flexibility and ultra-high resolution, it is apparent that scanning tunnelling microscopy is rapidly becoming the preferred technique for the elucidation of the details of surface structure down to atomic scales [13].

In this study, scanning tunnelling microscopy, combined with scanning electron microscopy, has been used to provide additional insight into the microstructural origin of the significant properties of the Tyranno (Si–Ti–C–O) fibre. The ultra-high-resolution STM topographical images obtained from the surfaces of both as-received and thermally desized Tyranno fibres, along with large-area three-dimensional SEM imaging, provide a clearer visualization of the surface structure of Tyranno fibre than has been possible hitherto.

## 2. Experimental procedure

### 2.1. Fibre samples

As-received Tyranno (Si–Ti–C–O) fibres (Grade E, UBE Industries Ltd) were supplied with a coating of surface size which can be removed thermally. These as-received fibres in consequence were heated, as specified by the fibre supplier, in air at ~ 500 °C for about 2 min to expose the uncoated surface. Hence, comparison of the sized and size-free fibres could be made. Thus, both Tyranno fibres in the as-received condition and after the thermal desizing treatment were examined by SEM and STM. It should be noted that, prior to examination as described, no further sample cleaning or preparation was used.

### 2.2. Scanning electron microscopy

SEM examination of the surface structure of the Tyranno (Si–Ti–C–O) fibres was carried out by using a Joel JSM-840 scanning electron microscope. A single bundle of the Tyranno fibre, containing some hundreds of individual filaments, was mounted on a standard SEM sample stud. Although the Tyranno fibres (Grade E in this study) are made from a relatively conductive material (specific resistance $10^2$–$10^3\ \Omega$ cm), sample-charging effects still can be seen in both size-coated and size-free Tyranno fibres exposed to beam voltages of 20–30 keV during SEM examination. Thus, the samples examined by SEM were sputter-coated, in the usual way, with a very thin layer of gold to prevent charging, prior to their final SEM examination.

### 2.3. Scanning tunnelling microscopy

The STM system used (W.A. Technology, Cambridge, UK) has been described in detail elsewhere [11, 12]. The tips used were produced from a 0.5 mm tungsten wire (99.99 %), by a routine electrochemical etch, in an aqueous 1 M KOH solution. By scanning the surfaces of both as-received and thermally desized Tyranno fibres, a large number of selfconsistent and reproducible STM images have been obtained in air in the constant current mode with a tunnel current typically of 1.0 nA and bias voltages ranging, in the experiments, from 200–1000 mV, sample positive or negative. Each image shown (256 pixels × 256 pixels) was generated in approximately 1 min 50 s. Similar images were also obtained, as indicated, but with different tips.

The STM images presented in this paper are subject only to the normal processing provided by the STM software, i.e. image fitting, image normalization and noise reduction; no other image corrections have been applied. Here, it should be noted that in order to enhance the topographical features described, some of the images shown have undergone image equalization processing, i.e. the image intensity data values of each pixel are adjusted up or down so that, in the final displayed image, there is an equal number of pixels of each resultant intensity.

Scanning tunnelling microscopy can also be used as a spectroscopic tool to provide electronic information,

e.g. tunnel current–voltage properties. The tunnel $I$–$V$ characteristics shown here were obtained with a constant tip–sample separation, set up by the initial scan parameters, via the sample-and-hold circuit in the STM feedback loop. The tip–sample bias voltage was increased step by step (up to 80 steps in the experiments) from a initially specified minimum to a chosen maximum, and at each sample point of bias voltage, the corresponding values of tunnel current were read repeatedly, typically eight times, recorded and averaged. Bias voltage control and data acquisition were under microcomputer control throughout this sequence. By setting the initial tunnel current and bias voltage in the experiments typically at 1.0 nA and 300 mV, respectively, a number of current–voltage curves were recorded at the positions selected both randomly and specifically on the surfaces of both as-received and thermally desized Tyranno fibres.

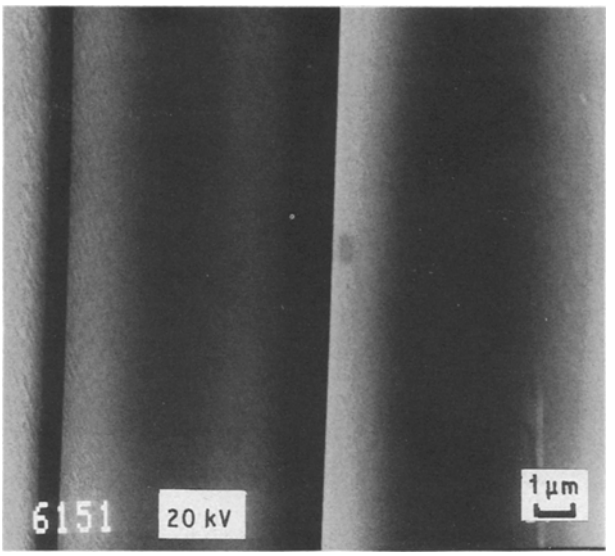


*Figure 1* An SEM image of the as-received Tyranno fibre showing individual filaments.

## 3. Results and discussion

### 3.1. Scanning electron microscopy

SEM examination of the as-received Tyranno fibres at low magnification indicates that these fibres are uniformly of one diameter ($\sim 9\,\mu m$), circular in shape, relatively smooth and featureless (Fig. 1). This is in agreement with the manufactured specification [2] and a previous SEM study [4]. The scanning electron micrographs at the same magnification of the thermally desized Tyranno fibres showed similar morphologies to those in Fig. 1 and therefore are not shown here.

Fig. 2a and b are, respectively, typical scanning electron micrographs at higher magnification obtained from the as-received and thermally desized Tyranno fibres. The size-coated surface of the as-received Tyranno fibre now shows somewhat ripple-like structure with no further indication of observable regular features. In contrast, the thermally desized Tyranno fibre surface clearly exhibits aligned individual or small bundles of micro-filaments. Furthermore, it can be seen from Fig. 2b that some of the micro-filaments in the centre of the image shown are rather smooth in form, while some, on the other hand, show tiny surface blemishes, circular or near circular. The micro-filaments indicated are estimated to be several tens of nanometres wide. Also, as shown in Fig. 2a and b, there are visible blemishes, large and small, on the outer surfaces of both fibre samples examined. These blemishes are attributed to the surface contaminants or the size-coating residues remaining on the surfaces of the fibres concerned.

### 3.2. Scanning tunnelling microscopy

Generally, scanning over a relatively large area, 500 nm × 500 nm, on the as-received Tyranno fibre surfaces, the STM images obtained at this scale did not show any significant topographical features because of the existence of the surface size overlayer. Sometimes these images were found to be distorted by the tip touching the protruding surface blemishes or spots, referred to above, on the sample surface or by the tip touching while scanning, local areas of the

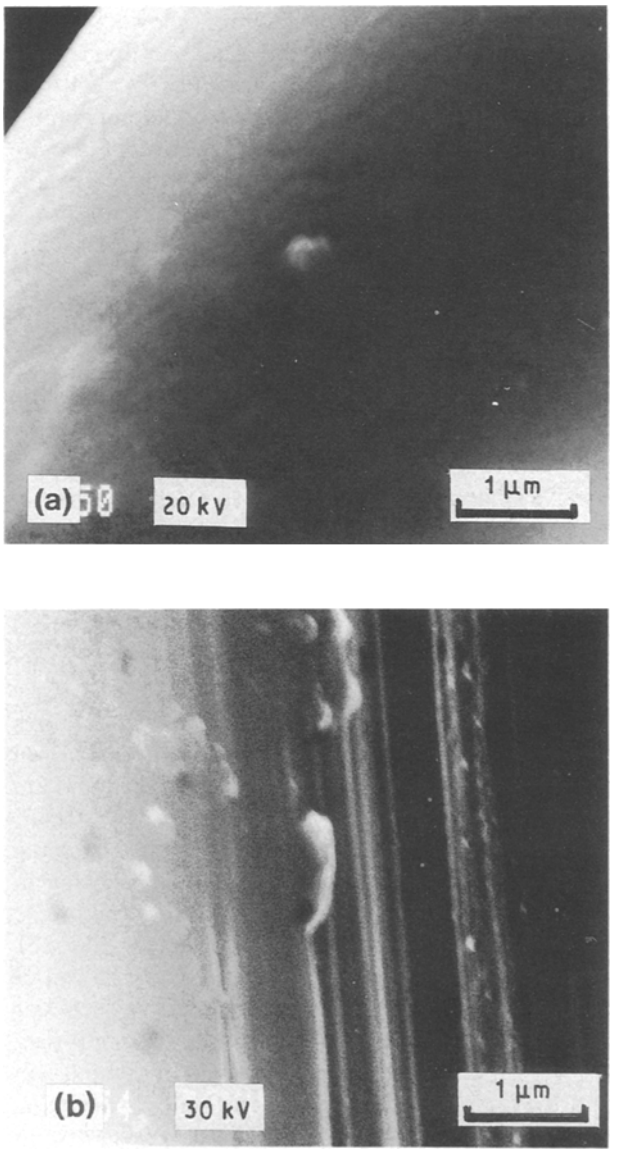


*Figure 2* Scanning electron micrographs of the Tyranno fibres (a) in the as-received condition, and (b) after the thermal desizing treatment.

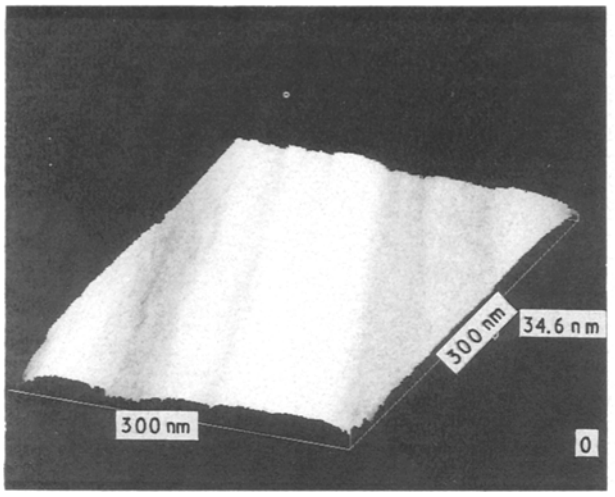


*Figure 3* One typical STM image (300 nm × 300 nm × 34.6 nm) of the as-received Tyranno fibre surface obtained at a bias voltage of 330 mV and a tunnel current of 1.0 nA showing micro-filamentary structure.

surface of poor electrical conductivity. However, through careful searching of the sample surface by moving the tip from one scanned area to another, some interesting structural features, showing micro-filamentary form (Fig. 3) and granular appearance (Fig. 4), could be observed repeatedly over relatively large and different scan areas located randomly on the fibres. The aligned micro-filaments shown in Fig. 3 are found to be more or less uniform in width, typically 48.50 nm, and the granular sizes in Fig. 4a are measured to be in the range 4.20–7.40 nm, typically 5.00 nm.

Occasionally, some fine topographical features could be observed by STM on the surface of the as-received Tyranno fibre over smaller scanned areas. Fig. 5 illustrates a typical example of one of these features alluded to, i.e. an overlapping layer structure. From Fig. 5, it can be seen that the overlapping distances of layers apparently vary greatly. Moreover, the overlapping layer heights, in the range 0.40–2.00 nm, are found to show little regularity, even when measured along a single layer, as imaged, from one end to another. In view of the topographical characteristics described, the overlapping layer structure is attributed to the presence of the surface size coating. In this instance then, these fine image features are not deemed to be characteristic of the actual surface structure of the Tyranno fibre studied and are not discussed further.

Figs 6 and 7 are the STM images obtained from the thermally desized Tyranno fibre surface, showing in some respects similar micro-filamentary structure to that in Fig. 3 or to the SEM images (see Fig. 2b). However, significant structural differences, as a consequence of the thermal removal of the surface size coating, are noted in the images of the sized and size-free Tyranno fibre surface examined. In comparison with the micro-filamentary structure shown in Fig. 3, these differences (shown in Figs 6 and 7) exist, first, in the shapes of micro-filaments, i.e. having a rather rough external surface including some cracks (more clearly displayed in Fig. 7), and second, in their widths,

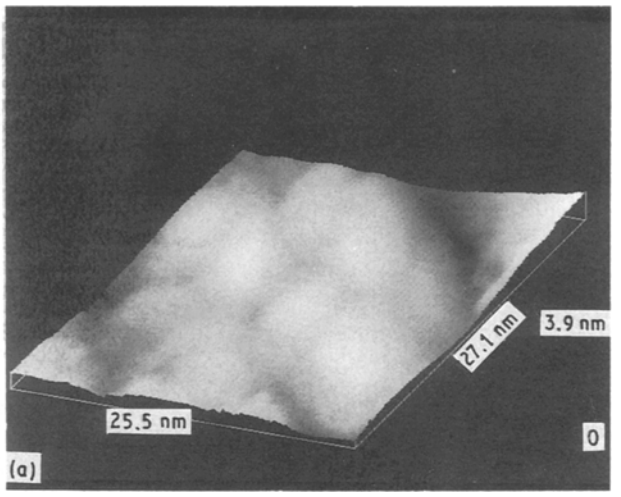


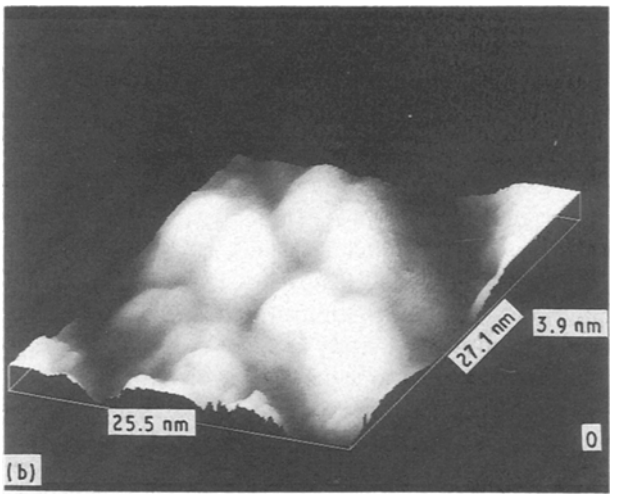


*Figure 4* Typical STM images (25.5 nm × 27.1 nm × 3.9 nm) of the as-received Tyranno fibre surface obtained at a bias voltage of 330 mV and a tunnel current of 1.0 nA: (a) showing granular structure and (b) the same image as (a) but with image equalization processing (see text).

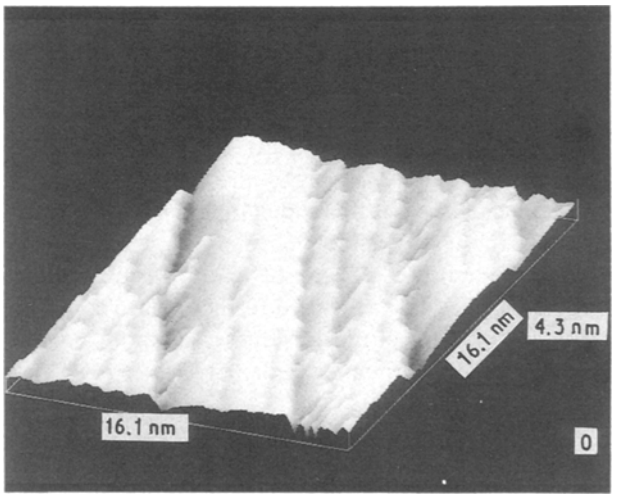


*Figure 5* An STM image (16.1 nm × 16.1 nm × 4.3 nm) of the as-received Tyranno fibre showing the overlapping layer structure (bias voltage 330 mV, tunnel current 1.0 nA).

i.e. varying from 30.00–70.00 nm. Furthermore, a granular structure with a size typically of 36.00 nm is found to exist on the right part of Fig. 6c, itself a high-magnification image taken from the right-upper cor-

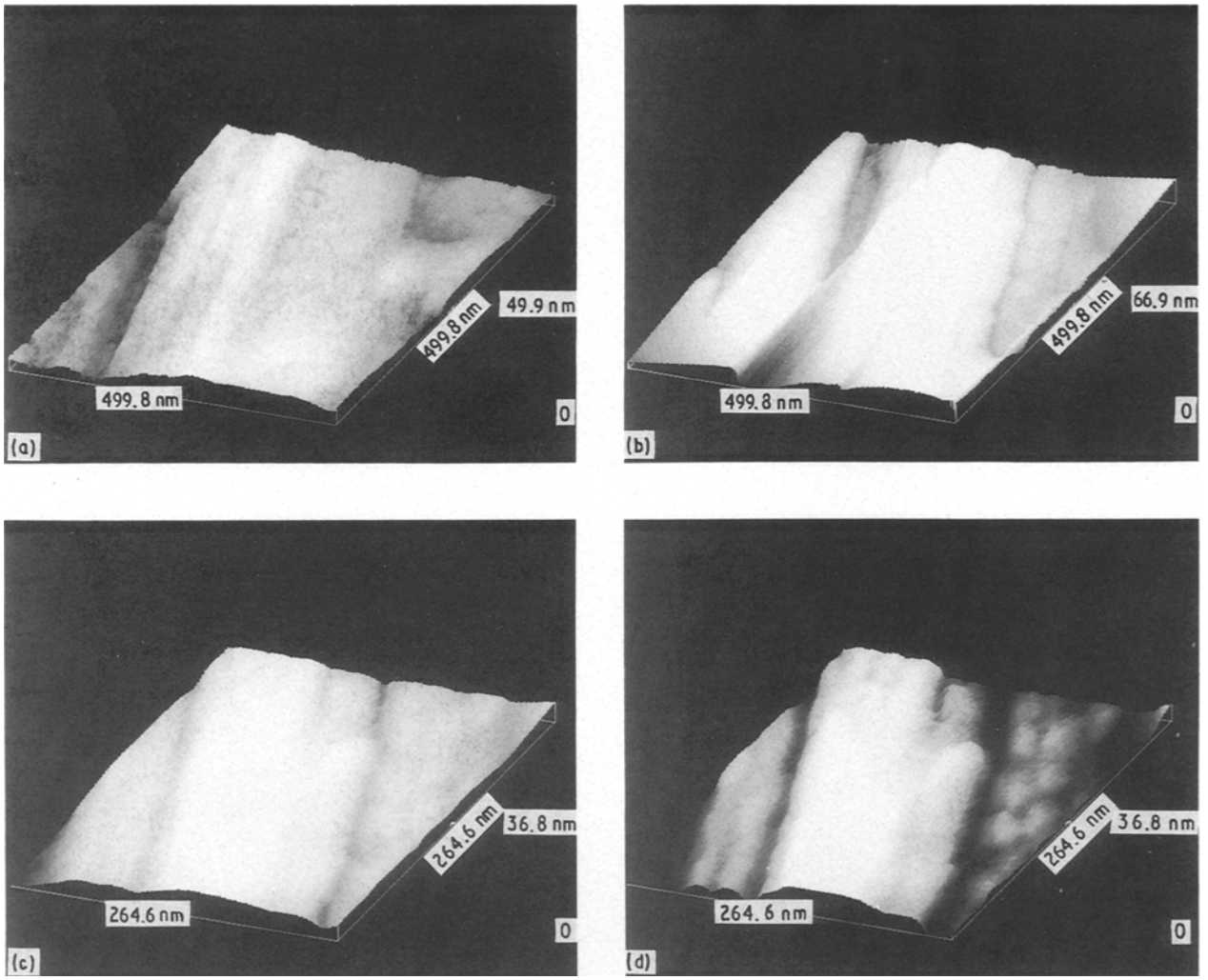


*Figure 6* Typical STM images of the thermally desized Tyranno fibre surface: (a) showing micro-filamentary structure over a 500 nm × 500 nm scan area (bias voltage 400 mV, tunnel current 1.4 nA); (b) showing micro-filamentary structure and granular structure over a 500 nm × 500 nm scan area (bias voltage 380 mV, tunnel current 1.0 nA); (c) the high-magnification image (264.6 nm × 264.6 nm × 36.8 nm) taken from the right-upper corner of (b), and (d) the same image as (c) but with the image equalization processing.

ner of Fig. 6b. On the other hand, a rather poorly defined granular structure, as shown in Fig. 8, frequently observed on certain positions of the thermally desized Tyranno fibre surface, is found to have a much smaller local granular size, typically, in the range 3.60 to 4.00 nm.

It is probable that the surface size coating when present may bury and hide to an extent the differences in the micro-filamentary widths and granular sizes found between the as-received and thermally desized Tyranno fibres. However, with the presumption that the thermal desizing treatment used is fully efficient and has little direct effect on the surface structure of the Tyranno fibre itself because of the low temperature used, the granules with a size as large as 36.00 nm in Fig. 6c cannot be simply attributed to the microcrystalline zones in the Si–Ti–C–O fibres [4, 5, 7]. In the various image searches conducted, these granular features in most cases are found either beside the aligned micro-filaments (Fig. 6c and d) or distributed among them (Fig. 7a and b). Furthermore, considering the fact that the apparent granular sizes are commensurate with the micro-filamentary widths and that these are located in definite areas aligned with the micro-filaments identified, the granular features shown in Figs. 6 and 7 are therefore thought to be locally fractured micro-filaments arising from the surface micro-texturing effects which occur during fibre processing or are induced by the size-coating residues remaining. On the other hand, the granular size in Fig. 8 is found to be larger than the typical crystallite size ( < 2.00 nm), as determined by X-ray diffraction [4, 5, 7]. The small crystallite sizes derived in the latter are thought likely to be associated with the possible contributions of lattice distortions, i.e. oxygen dispersed within the β-SiC tetrahedral structural units [3, 4]. In addition, assuming the granules observed by STM and the X-ray microcrystallite sizes are related, it should be noted here that scanning tunnelling microscopy, with patience, can measure the actual distribution of the granular sizes concerned, whereas X-ray diffraction can only give a microcrystallite mean value, because the X-ray beam samples a significantly larger sample cross-section than does the STM experiment [14].

Furthermore, when scanning within the individual granules or on the micro-filamentary areas, no specific organized structure at an atomic scale could be resolved by STM, probably because of the effects of the excess oxygen introduced in the curing process on the

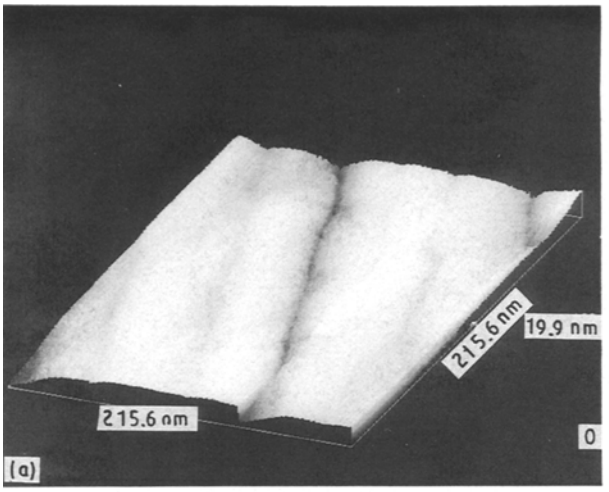


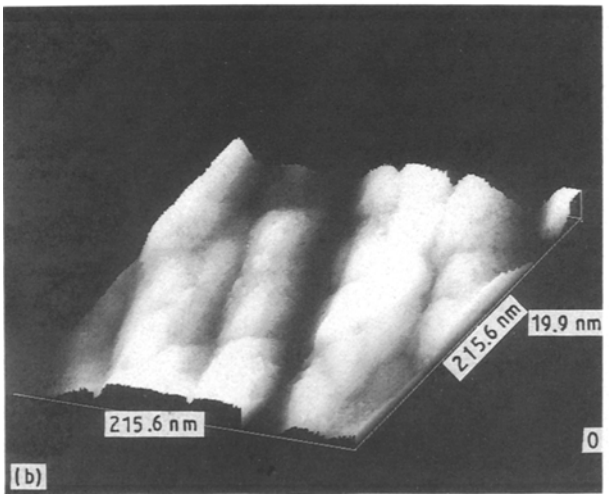


*Figure 7* An STM image (215.6 nm × 215.6 nm × 19.9 nm) of the thermally desized Tyranno fibre surface obtained at a bias voltage of 380 mV and a tunnel current of 1.0 nA: (a) showing rough surfaces of micro-filaments, and (b) an image of (a) processed by equalization.

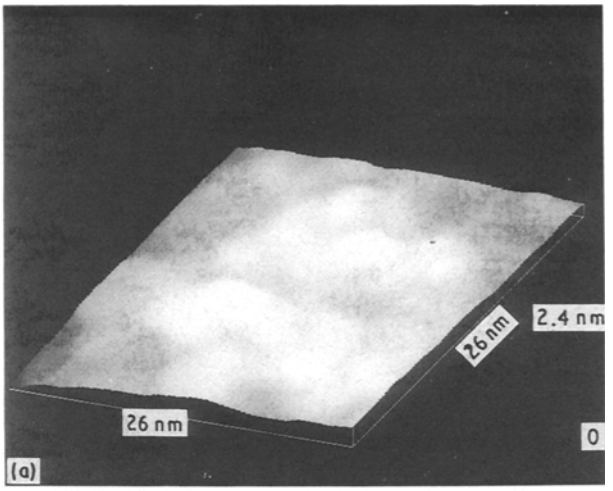


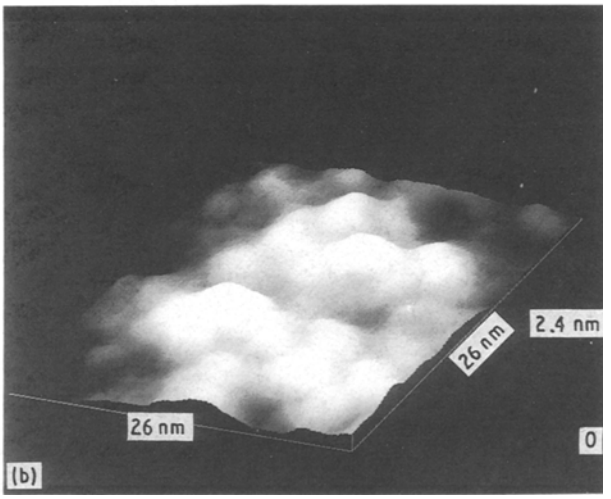


*Figure 8* One typical STM image (26.0 nm × 26.0 nm × 2.4 nm) of the thermally desized Tyranno fibre surface obtained at a bias voltage of 380 mV and a tunnel current of 1.0 nA: (a) showing rather poorly defined granular structure and (b) an image of (a) processed by equalization.

microcrystalline state, e.g. inducing many SiC phases in the Tyranno fibres [3, 6]. Likewise, this is probably the reason why the granular structure observed on the surfaces of the thermally desized Tyranno fibres is poorly defined in the STM images.

Fig. 9 is a typical STM image showing another kind of micro-filamentary, or more precisely, fibrillar structure frequently observed on the surfaces of the thermally desized Tyranno fibre. From Fig. 9b, a high-magnification image taken from the centre right part of Fig. 9a, it can be seen clearly that ultra-small micro-filaments or fibrils lie curved on the fibre surface with an extremely narrow width when compared with the micro-filaments described above. The widths of these smallest resolved linear structures are thus measured to be 1.30–1.80 nm, typically 1.50 nm. The spacings between two narrow micro-filaments are in contrast found to be 1.70–2.40 nm, typically 1.90 nm.

In this regard, it is known that the precursor polytitanocarbosilane (PTC) structure is composed of polycarbosilane chains crossed-linked by $-O-Ti(OBu)_x-O-$ ($x = 0, 1, 2$) units [2, 8]. The conversion of PTC polymer chains into inorganic Si–Ti–C–O fibres, in the processing of the Tyranno fibre [2], occurs during continuous high-temperature heating in a non-oxidizing atmosphere. Even though during pyrolysis, a dramatic consolidation and densification of the fibre arises, given the sizes of the ultra-fine features alluded to above, it is very tempting to associate the presence of the tiny micro-filaments, as shown in Fig. 9, with the PTC or PC polymeric chains in the Tyranno fibres [14, 15]. If so, then some of the general polymeric structural features of the precursor polymer matrix are retained in the final Tyranno fibre after pyrolysis and may thus affect the ultimate properties of the fibre formed.

Finally, it is noted that the microcrystalline graphitic structure observed by high-resolution TEM in SiC fibres [16] and found to be present in polymer-pyrolysed ceramic fibres by Raman spectroscopy [17] was never observed by STM, in spite of much effort in the work described here, on the surfaces of the thermally desized Tyranno fibre. This lack of detectable graphitic character suggests that any graphitic carbon present in the fibre must be confined to extremely small and well separated regions; if otherwise, the graphitic

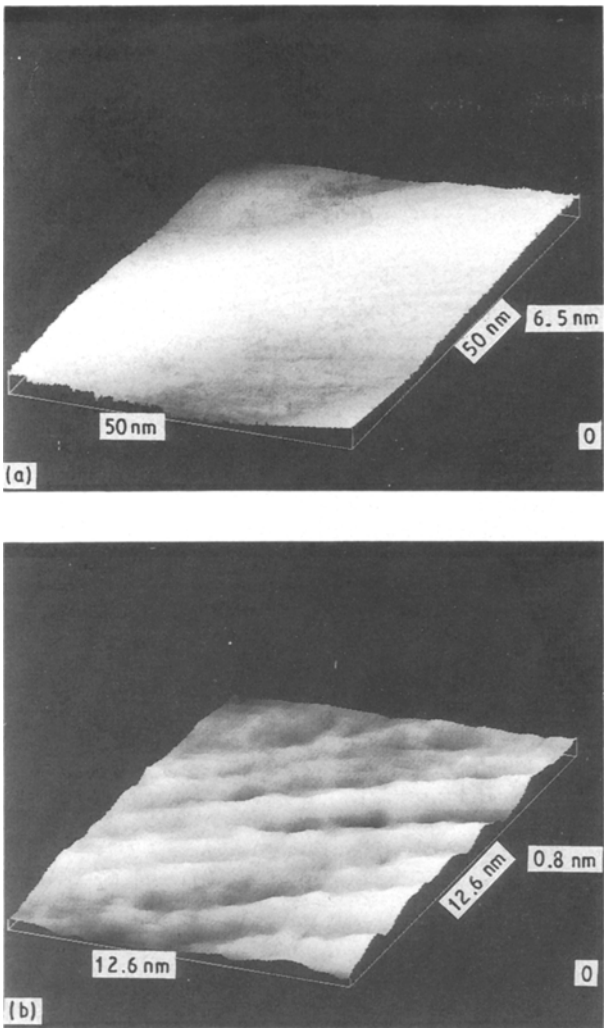


*Figure 9* A typical STM image obtained from the thermally desized Tyranno fibre surface at a bias voltage of 500 mV and a tunnel current of 1.0 nA: (a) showing narrow and curved micro-filaments (image dimension: 50.0 nm × 50.0 nm × 6.5 nm), and (b) a high magnification image (12.6 nm × 12.6 nm × 0.8 nm) taken from the centre right part of (a).

structure alluded to would have been found. Thus, most of the carbon present in the fibre is likely to be in the carbidic form, i.e. Si–C or Ti–C.

### 3.3. STM tunnel current versus bias voltage characteristics

The $I$–$V$ characteristics obtained in an ambient air condition can be rather variable. However, those obtained for the as-received Tyranno fibre surfaces studied show nearly identical behaviour and independence of the position on the sample surface. Those similarly obtained for the thermally desized Tyranno fibre surfaces show slight but significant differences and are again consistent from point to point. Fig. 10 is representative of a group of $I$–$V$ plots obtained at the surface of the as-received and thermally desized Tyranno fibre. As can be seen, the $I$–$V$ curves in Fig. 10 are asymmetrical about zero bias voltage, exhibiting a slight rectifying effect. This rectifying effect is manifest as a larger current at a particular negative bias voltage than at the same positive bias voltage. However, it should be noted that in the case of the as-

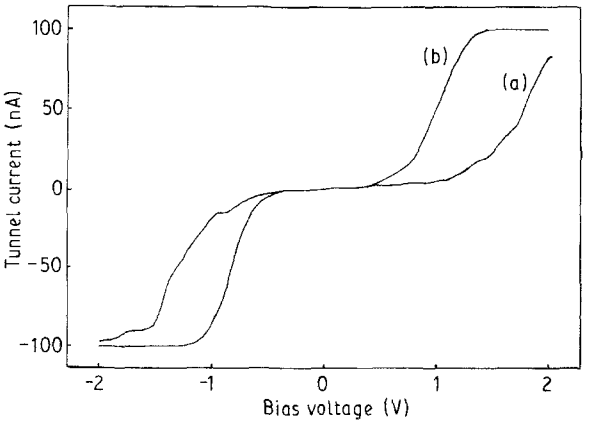


*Figure 10* The tunnel current versus voltage characteristics for (a) the as-received, and (b) the thermally desized Tyranno fibre surfaces.

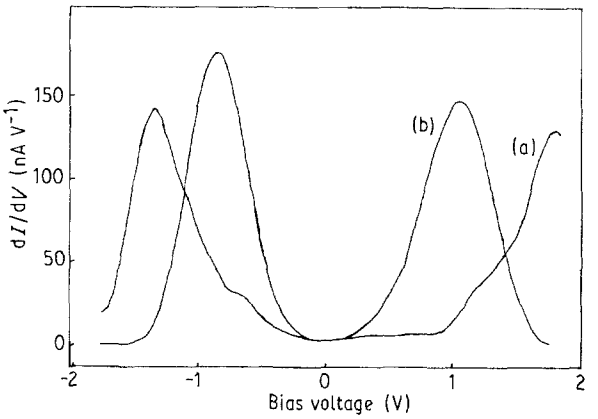


*Figure 11* The corresponding differential conductance versus voltage curves for (a) the as-received and (b) the thermally desized Tyranno fibre surfaces.

received Tyranno fibre, the tunnel current becomes constant for the bias voltage above $-1.20$ and $+1.40$ V, which is probably due to the onset of actual electron emission at the tip. Here, the rectification behaviour seen is believed to arise mainly from the different transmission probabilities caused by asymmetric barrier shape for the negative and positive bias [18].

Fig. 11 shows plots of the differential conductance versus voltage derived from the $I$–$V$ characteristics shown in Fig. 10. Now, it can be seen clearly that the dependence of the differential conductance on voltage for the two sample surfaces studied are different in both peak heights and peak positions. It is known that the scanning tunnelling spectroscopy obtained is related, under certain conditions, to the local density of states of the sample surface [19]. However, without good knowledge of the local surface density of states determined by other surface analysis techniques or by theoretical calculations and additional complexity of surface adsorption effects in air, it is difficult at present to define particularly the peaks shown in Fig. 11. Further work needs to be done in this regard under UHV STM conditions. Nevertheless, it is obvious that the $I$–$V$ properties of the as-received and thermally desized Tyranno fibres are generally different, perhaps not surprisingly.

## 4. Conclusions

Scanning tunnelling microscopy with ultra-high resolution, combined with conventional scanning electron microscopy, has been used to study the details of the surface structure of the Tyranno (Si–Ti–C–O) fibres in the as-received condition and after thermal desizing treatment. The direct visualization of the surface structure of the Tyranno fibre via STM and SEM reveals clearly the structural similarities and differences between the as-received and thermally desized Tyranno fibres. As a consequence of the removal of the coating of surface size from the as-received Tyranno fibre, the micro-filamentary structure and the granular structure observed by STM are found to be significantly different in their topographical shape and size, i.e. the micro-filaments observed show rough surfaces with some fractures and the granular structure is poorly defined. No ordered structure at atomic resolution was resolved on the thermally desized Tyranno fibre surface. On the basis of these initial results, the surface structure of the Tyranno fibre studied can be characterized as non-crystalline and amorphous. In addition, extremely narrow and curved micro-filaments observed on the thermally desized Tyranno fibre surfaces by STM are believed to reflect the structure of the precursor polymeric chains retained in the fibre after processing. Finally, the scanning tunnelling spectroscopy done shows differences in the $I$–$V$ properties between the as-received Tyranno fibre and the thermally desized Tyranno fibre.

The work presented here is a prelude to further STM studies of the effects of processing heat treatment, the role of the structure and properties of polymer precursor materials on the pyrolysis product and how these affect, via fibre fabrication, the surface structure of the Tyranno (Si–Ti–C–O) fibres of interest and their local electronic properties.


## Acknowledgements

One of the authors (H. X. You) thanks the University of Ulster for a postgraduate research studentship. Thanks are also due to the IRCSS, University of Liverpool, for support. The authors thank Dr Steve Lowry, Department of Biological and Biomedical Sciences, for the scanning electron microscope images and Mr S. Davis, UBE Europe GmbH Ltd (London office), for the supply of Tyranno fibre samples.


## References


1. S. YAJIMA, T. IWAI, T. YAMAMURA, K. OKAMURA and Y. HASEGAWA, *J. Mater. Sci.* **16** (1981) 1349.
2. T. YAMAMURA, Technical Report of Ube Industries Ltd.
3. V. S. R. MURTHY, M. H. LEWIS, M. E. SMITH and R. DUPREE, *Mater. Lett.* **8** (1989) 263.
4. D. B. FISCHBACH, P. M. LEMOINE and G. V. YEN, *J. Mater. Sci.* **23** (1988) 987.
5. T. YAMAMURA, T. ISHIKAWA, M. SHIBUYA, T. HISAYUKI and K. OKAMURA, *ibid.* **23** (1988) 2589.
6. F. BABONNEAU, G. D. SORARU and J. D. MACKENZIE, *ibid.* **25** (1990) 3664.
7. Y.-C. SONG, Y. HASEGAWA, S.-J. YANG and M. SATO, *ibid.* **23** (1988) 1911.
8. Y. SONG, C. FENG, Z. TAN and Y. LU, *J. Mater. Sci. Lett.* **9** (1990) 1310.
9. J. K. GIMZEWSKI and A. HUNBERT, *IBM J. Res. Develop.* **30** (1986) 472.
10. G. BINNIG, H. ROHER, CH. GERBER and E. WEIBEL, *Phys. Rev. Lett.* **49** (1982) 57.
11. N. M. D. BROWN and H. X. YOU, *Surf. Sci.* **237** (1990) 273.
12. N. M. D. BROWN, G. M. TAGGART and H. X. YOU, *J. Mater. Sci.* **26** (1991) 4971.
13. P. K. HANSMA and J. TERSOFF, *J. Appl. Phys.* **61** (1987) R1.
14. N. M. D. BROWN and H. X. YOU, *J. Mater. Chem.* **1** (1991).
15. L. PORTE and A. SARTRE, *J. Mater. Sci.* **24** (1989) 271.
16. S. YAJIMA, K. OKAMURA, T. MATSUZAWA, Y. HASEGAWA and T. SHISHIDO, *Nature* **279** (1979) 706.
17. J. LIPOWITZ, H. A. FREEMAN, R. T. CHEN and E. R. PRACK, *Adv. Ceram. Mater.* **2** (1987) 121.
18. A. A. LUCAS, P. H. CULTER, T. E. FEUCHTWANG, T. T. TSONG and T. E. SULLIVAN, *J. Vac. Sci. Technol.* **A6** (1988) 461.
19. N. D. LANG, *Phys. Rev.* **B34** (1986) 5947.



*Received 23 October 1991*
*and accepted 21 May 1992*